



## Preparation and Properties of PP Composites Containing $\gamma$ -Aminopropyltriethoxysilane-Modified Tourmaline

Guangtao Zhang<sup>1,\*</sup>, Andrii Bieliatynskiy<sup>1</sup>, Dinghao Wang<sup>1</sup>, Mingyang Ta<sup>1</sup> and Yajian Deng<sup>1</sup>

<sup>1</sup> North Minzu University School of Civil Engineering, Yinchuan, 750021, NingXia, China

**SUMMARY:** *In order to improve the interfacial compatibility between tourmaline (TP) and polypropylene (PP) matrix, and to improve the mechanical properties of TP/PP composites, in this study,  $\gamma$ -aminopropyltriethoxysilane (KH550) was used as a modifier to modify the surface of TP and the modified TP/PP composite was prepared by melt blending and injection molding process. The mechanical property tests showed that the tensile and flexural properties of the composites were improved to a certain extent; the 1% concentration of KH550 modifier had the best modification effect. When the content of tourmaline was 10 wt%, the tensile strength of the composites was increased by 16.87% (compared with that of the pure PP, the tensile strength was increased by 31.23%). When the content of modified TP was 5 wt%, the flexural strength of the composites was increased by 9.42% (compared with that of the pure PP). 9.42% (15.2% increase over pure PP). Microstructural analysis (SEM) showed that the modification with 1 % concentration of KH550 could effectively inhibit the agglomeration of TP and improve its dispersion and bonding in PP matrix, thus exerting the reinforcing effect of inorganic filler reinforcement.*

**KEYWORDS:** *tourmaline modification; polypropylene; composites; silane coupling agent; mechanical properties*

## 1 Introduction

Polypropylene (PP) is a thermoplastic addition polymer made from a combination of propylene monomers and a typical non-polar, chemically inert polymer. Polypropylene (PP) is used in a wide range of applications, including consumer packaging, plastic parts for the automotive industry, and textiles, because of its good all-around properties, low density, good corrosion and heat resistance, and simple processing conditions. Polypropylene (PP), as one of the three major general-purpose resins, has an increasing industrial demand, but its mechanical properties are insufficient, resulting in certain limitations in its application[1], so the use of inorganic fillers filled with polypropylene to expand the application scenarios has become very necessary in order to meet the future needs of science and technology[2].

Tourmaline (TP) is a cyclic structure of aluminum, sodium, iron, magnesium and lithium containing boron characterized by the silicate mineral. Tourmaline has unique physicochemical properties due to its complex chemical composition and crystal structure, mainly spontaneous polarization, thermoelectricity, release of negative ions, far-infrared radiation, etc. It is used in environmental protection, medical and health care, catalysis, and other research fields[3-6].

TP is extremely prone to agglomeration problems during processing due to its large specific surface area and high specific surface energy[7]. In this study, TP was modified by selecting  $\gamma$ -

\*clngtao2000@163.com

<https://doi.org/10.65102/is20261268>

aminopropyltriethoxysilane (KH550) modifier with different concentrations to improve its dispersion and compatibility in PP matrix [8-10], the modified TP was mixed with PP and according to a certain ratio, and the composites with PP as the matrix and modified TP as the reinforcement were produced through melt blending and injection molding process, and the modified TP and composites were tested for macroscopic mechanical properties. and composites were tested for macro mechanical properties and characterized by microscopic tests.

## 2 Experimental part

### 2.1 Main raw materials

Polypropylene (PP), Nordic Chemical RB206MO; Tourmaline powder (TP), 400 mesh, Jingwei Mineral Processing Factory, Lingshou County, Hebei Province; anhydrous ethanol, analytically pure, Foshan Shanlong Chemical Co.

Table 1: Fly ash bead composition list (Unit: %)

SiO <sub>2</sub>	Fe <sub>2</sub> O <sub>3</sub>	Al <sub>2</sub> O <sub>3</sub>	MgO	CaO	Na <sub>2</sub> O	TiO <sub>2</sub>	K <sub>2</sub> O	MnO	CuO	ZrO <sub>2</sub>
42.74	23.91	21.9	4.56	2.53	2.36	0.809	0.222	0.172	0.158	0.11

### 2.2 Instruments and equipment

Microcomputer gantry tester, KY-D4105, Shanghai Horiyang Precision Measuring Instrument Co., Ltd; desktop vertical injection molding machine, Z-0020g, RCZJ, China; Fourier Transform Infrared Spectrometer (FTIR), Scientific Nicolet iS20, Thermo Fisher, U.S.A.; Contact Angle/Surface Tension Meter, SZ-CAMC32, Shanghai Xuanzhun; X-ray Diffractometer (XRD), D8 Advance, Bruin, Germany; X-ray Diffraction (XRD), D8 Advance, Bruin, Germany CAMC32, Shanghai Xuanzhun Company; X-ray diffractometer (XRD), D8 Advance, Bruker Company, Germany; scanning electron microscope (SEM), SIGMA-360, ZEISS Company, Germany; comprehensive thermal analyzer, STA200, HITACHI Company, Japan.

### 2.3 Sample Preparation

#### 2.3.1 TP surface modification

Firstly, TP was dried in a preheated oven at 80°C for 2h, and then anhydrous ethanol and deionized water were mixed proportionally as the diluent, and the KH550 modifier solutions with concentrations (mass fraction of solvent) of 1%, 2%, and 3% were proportionally configured (0% KH550 represented the control group of the unmodified test), and then the samples were heated to 60°C and stirred magnetically for 30min, and then cleaned and pump-filtered with ethanol and deionized water. Deionized water cleaning, pumping filtration, the processed powder placed in the oven drying 12h.

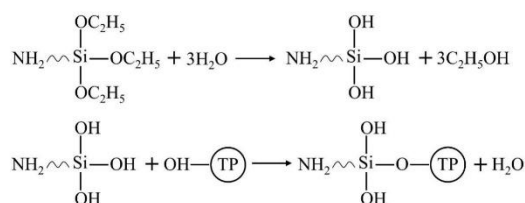


Figure 1: Schematic Diagram of the Mechanism of Action of KH550 Modified TP

### 2.3.2 Preparation of TP/PP composites

Firstly, PP is put into the oven to dry at 80°C for 2h, then PP and TP are put into the high-speed mixer at 2000r for 10min, and then the obtained materials are put into the twin-screw extruder to be extruded at the temperature of 180-190°C in the heating section, and the speed of the screw of the host machine is 30r/min, and the speed of the charging material is 25r/min. Table 2 is the formula of the composite material, and according to the formula of Table 2, the silane coupling agent KH550 will be modified TP and PP, and the composite material will be made of TP and PP, which are modified TP and PP. Modified TP and PP by high-speed mixer after mixing the material slowly into the feed port, through the melt blending method to make raw materials from the glass state into a viscous flow state with the head was extruded, and after artificial traction to the liquid-cooled circulating device into the pelletizer will be cut into 3 ~ 5mm fine particles. The granules are evenly put into the desktop injection molding machine 230°C, 27MPa to make standard tensile and bending test samples.

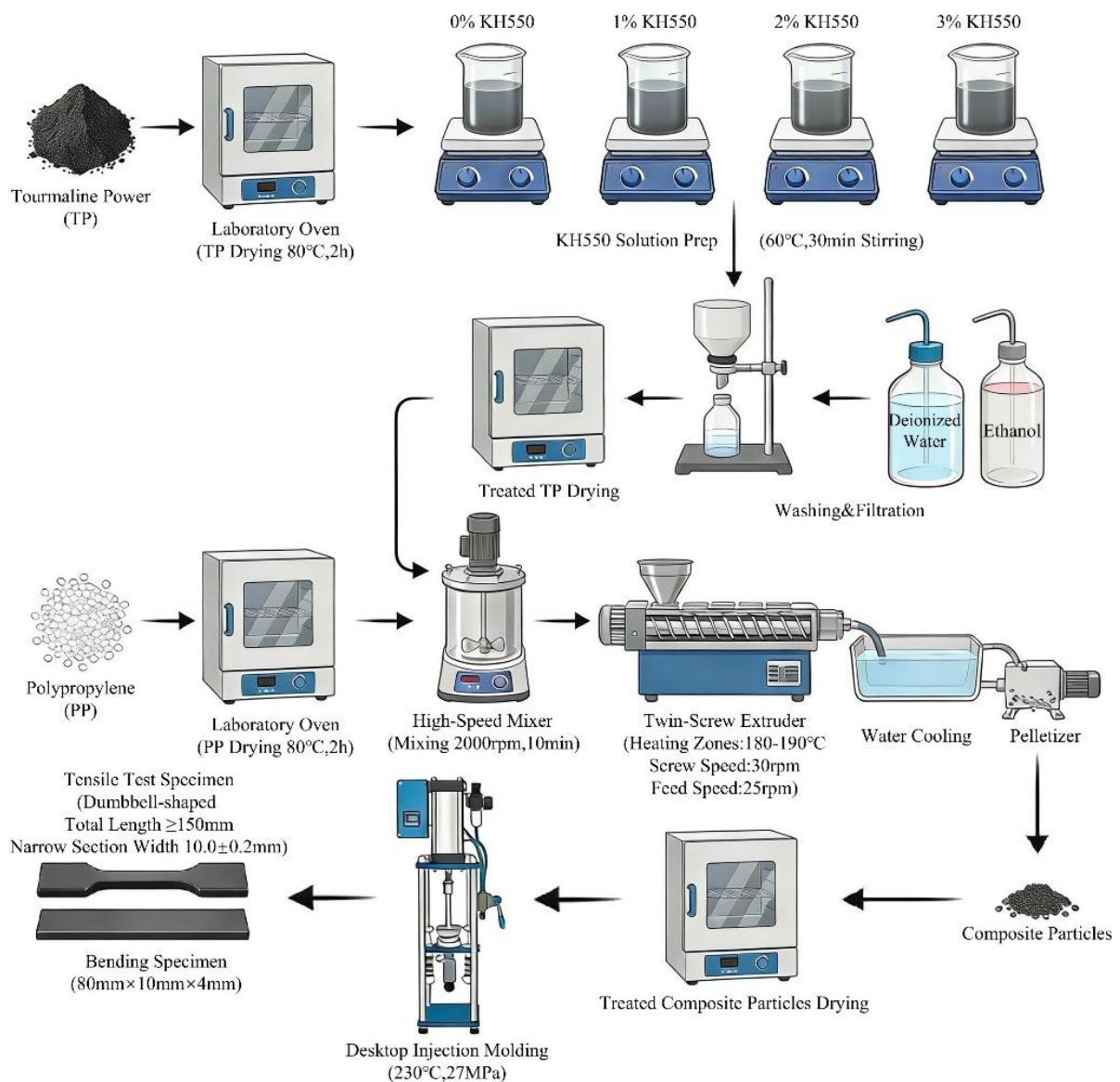


Figure 2: Process for Preparing KH550 Modified TP and TP/PP Composite Materials



Figure 3: Composite specimens

Table 2: Modified TP composite formulations (Unit:%)

Formulation	KH550 concentration (wt%)	PP (wt%)	KH550-TP (wt%)
1	0	95	5
2		90	10
3		85	15
4		80	20
5	1	95	5
6		90	10
7		85	15
8		80	20
9	2	95	5
10		90	10
11		85	15
12		80	20
13	3	95	5
14		90	10
15		85	15
16		80	20

### 3 Performance testing and characterization

FTIR test: Fourier Transform Infrared Spectroscopy was used to observe the changes in functional groups of tourmaline powder. Dried potassium bromide was chosen to be mixed with the sample and pressed, the scanning range was 400-4000  $\text{cm}^{-1}$  and the number of scans was 32.

Contact Angle Determination: The contact angle between the material and water was determined by using a tablet press to make the sample into a cake-like specimen.

XRD characterization: Cu target  $K\alpha$  rays, scanning range  $5^{\circ}$ - $80^{\circ}$ , scanning speed  $2^{\circ}/\text{min}$ .

SEM analysis: The impact sections of the composites were tested using a scanning electron microscope. The prepared experimental samples were punched off by the impact testing machine, the impact section was protected, and the quenched section was sprayed with gold for 120s, and then observed and photographed, during which the accelerating voltage was 5kV.

Mechanical properties test: tensile strength in accordance with GB/T1040.2-2006 test, running speed 50mm/min; bending strength in accordance with GB/T9341-2008 (three-point bending) test, running speed 10mm/min.

Thermal stability test:  $\text{N}_2$  atmosphere, set the temperature range of 30-800  $^{\circ}\text{C}$ , the rate of

temperature increase rate of  $10\text{ }^{\circ}\text{C} / \text{min}$ .

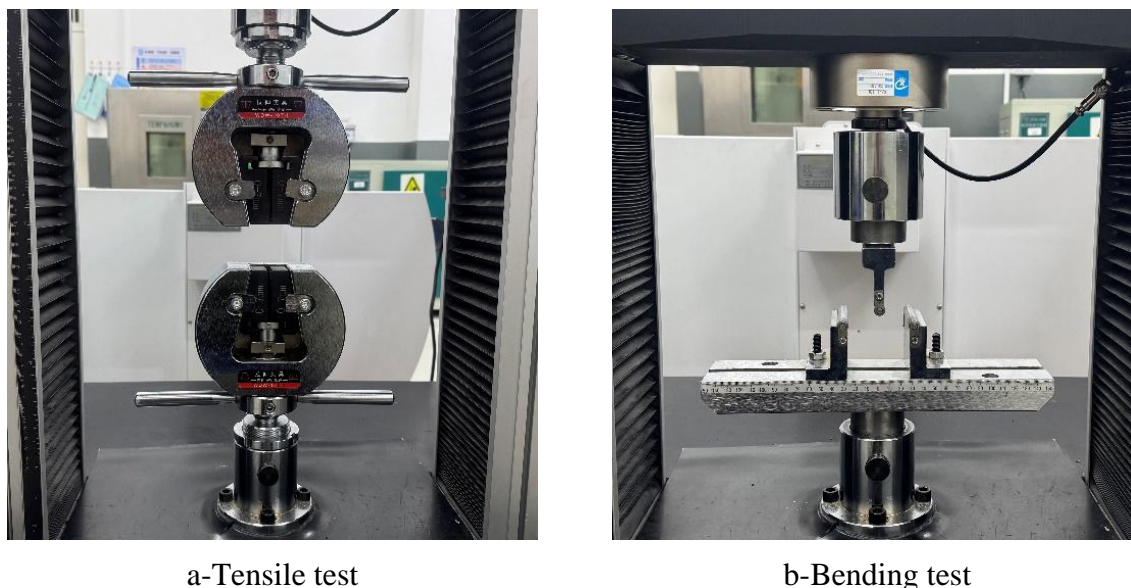


Figure 4: Experimental equipment for mechanical property test

## 4 Results and discussion

### 4.1 TP modification effect

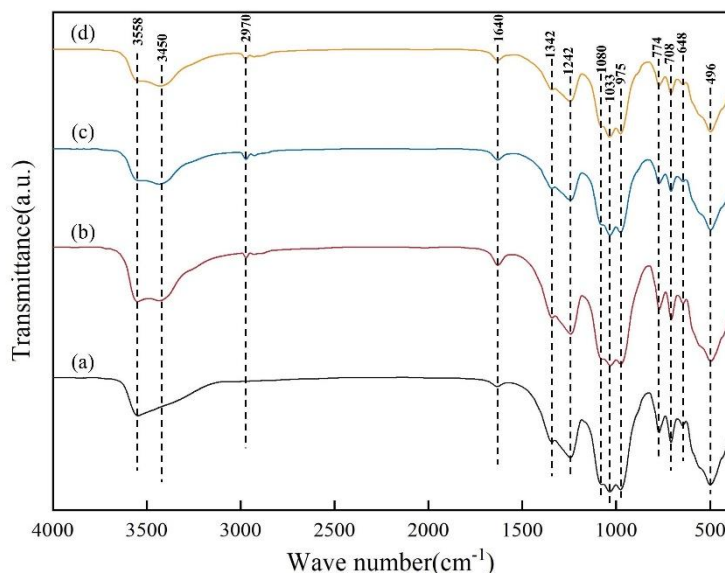
#### 4.1.1 FT-IR analysis

Figure 5 shows the FT-IR diagrams of TP modified by different KH550 modifier concentrations. The infrared absorption spectrum of TP is mainly composed of  $[\text{SiO}_{(4)}]$  ionophore,  $[\text{BO}_3]$  atomophore,  $[-\text{OH}]$  hydroxyl group, water and octahedral cation M-O vibration, and the main composition of TP is complex, and its composition and atomic composition change with geological conditions and formation, so the infrared spectra of different types of TP will differ. spectra of different types of TPs are different.

From Fig. 5(a), it can be seen that there are  $[-\text{OH}]$  hydroxyl stretching vibration peaks at  $3558\text{ cm}^{-1}$  and  $[-\text{OH}]$  hydroxyl bending vibration peaks at  $1640\text{ cm}^{-1}$  in unmodified TP, indicating the presence of water molecules in TP; the presence of B-O bonding stretching vibration peaks at  $1342\text{ cm}^{-1}$  and  $1242\text{ cm}^{-1}$  indicates the presence of  $[\text{BO}_3]$  groups;  $1080\text{ cm}^{-1}$ ,  $1080\text{ cm}^{-1}$ ,  $1242\text{ cm}^{-1}$  and  $1242\text{ cm}^{-1}$  indicate that there is no water molecules in TP; and the presence of B-O bonding stretching vibration peaks at  $1080\text{ cm}^{-1}$  and  $1242\text{ cm}^{-1}$  indicates that there is a water molecule in TP. The presence of asymmetric stretching vibrational peaks of Si-O-Si at  $1080\text{ cm}^{-1}$ ,  $1033\text{ cm}^{-1}$ , and  $975\text{ cm}^{-1}$  and symmetric stretching vibrational peaks of Si-O-Si at  $774\text{ cm}^{-1}$ ,  $708\text{ cm}^{-1}$ , and  $648\text{ cm}^{-1}$  indicate the presence of  $[\text{SiO}_{(4)}]$  ions; the presence of a vibrational peak of M-O at  $496\text{ cm}^{-1}$  indicates the presence of octahedral ions. O vibrational peak at  $496\text{ cm}^{-1}$ , indicating the presence of the octahedral cation M-O. The samples used in this experiment conformed to the infrared absorption spectral characteristics of TP, which coincided with the characteristic composition of TP.

Figures 5(b), 5(c), and 5(d) show the FT-IR maps of TP modified with three different KH550 concentrations, respectively, and the positions of the peaks are basically close to those in Fig. 5(a), with the difference that two absorption peaks are added at  $3450\text{ cm}^{-1}$  and  $2970\text{ cm}^{-1}$ , among which the telescopic vibrational peaks of the  $[-\text{NH}_{(2)}]$  amino group are found at  $3450\text{ cm}^{-1}$ , the

telescopic vibrational peaks of [-NH<sub>2</sub>]<sub>2</sub>amino group at 2970 cm<sup>-1</sup>, the telescopic peaks of [-NH<sub>2</sub>]<sub>2</sub>amino group at 2970 cm<sup>-1</sup>, and the telescopic peaks of [-NH<sub>2</sub>]<sub>2</sub>amino group at 2970 cm<sup>-1</sup>, which is the most important one. The saturated C-H stretching vibration peak at 2970 cm<sup>-1</sup>. This proves that the chemisorption of KH550 on the surface of TP occurred due to chemical bonding, which led to the generation of new absorption peaks on the modified TP, further proving that KH550 aggregated on the surface of TP and modified TP.

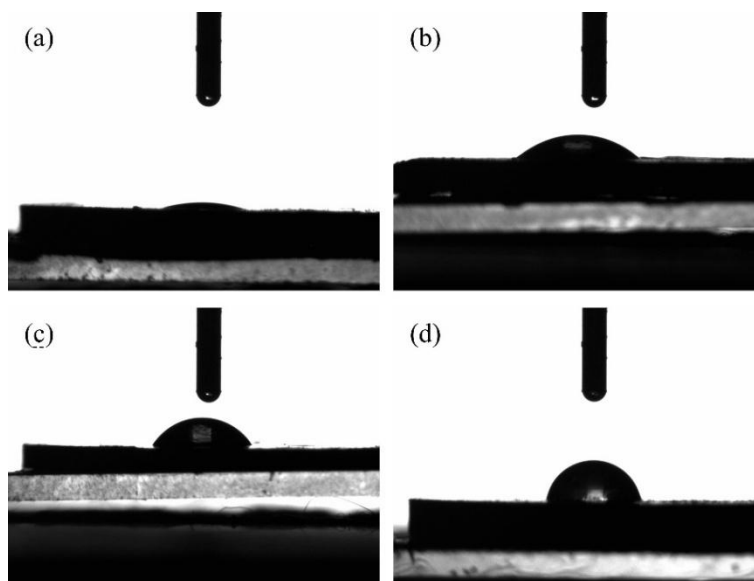


a-0% KH550-TP;b-1% KH550-TP;c-2% KH550-TP;d-3% KH550-TP

Figure 5: FT-IR spectra of TP modified with different concentrations of KH550 modifier

#### 4.1.2 Contact angle analysis

The contact angle is the angle between the direction of the combined force of the surface tension of the liquid and the surface tension of the solid and the solid surface at the junction of the solid, liquid and gas phases. During the test, the contact angle of the modified TP with different concentrations was measured to be 10.86° [see Fig. 6(a)], 41.78° [see Fig. 6(b)], 60° [see Fig. 6(c)], and 82.6° [see Fig. 6(d)], respectively, with water drops from the water contact angle tester feeder to the specimen powder after the press. The contact angle increased with the increase in the concentration of the modifier, indicating the enhanced hydrophobicity of the modified TP. Among them, the contact angle increased by 30.92° when the concentration of modifier was changed from 0% to 1%. This is because the hydrolysis of KH550 produces active silanol groups (-Si-OH) and the free hydroxyl groups (Si-OH)/(M-OH) on the surface of TP after dehydration condensation to form (Si-O-Si)/(Si-O-M) covalent bonds, so that the surface of the TP is wrapped by KH550, and the polar hydroxyl groups are consumed and the contact angle is increased; the contact angle is increased when the concentration of the modifier is increased from 1% to 2%, 2% to 3%, and 2% to 3%, respectively. 3% the contact angle increased by 18.22° and 22.6°, respectively, with little difference in the angle of change. This is because when an excess of KH550 was introduced, unreacted KH550 molecules aggregated on the surface of TP, and the dehydration and condensation of the excess silanol groups (-Si-OH) to form a siloxane network, which caused the contact angle to continue to increase[11].

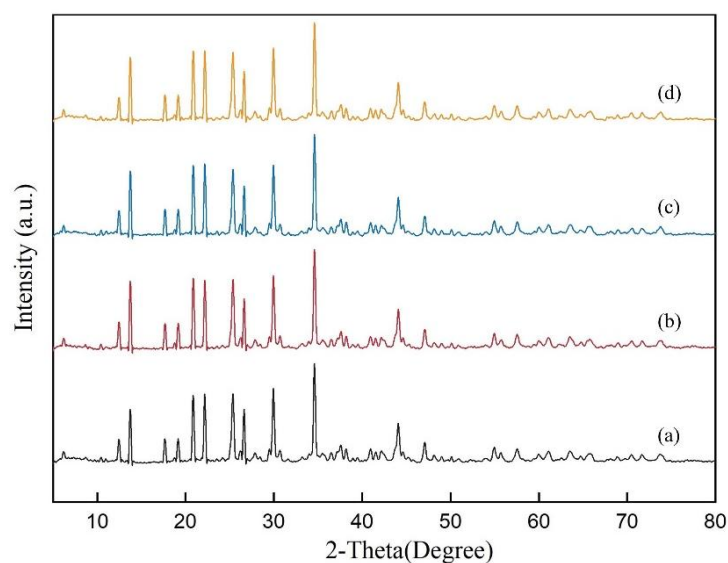


a-0% KH550-TP; b-1% KH550-TP; c-2% KH550-TP; d-3% KH550-TP

Figure 6: Contact angle of TP modified with different concentrations of KH550 modifier

#### 4.1.3 XRD analysis

Figure 7 shows the XRD patterns of TP modified with different concentrations of KH550 modifier. The main peaks of unmodified TP were located at  $2\theta$  angles of  $12.38^\circ$ ,  $13.75^\circ$ ,  $17.65^\circ$ ,  $18.83^\circ$ ,  $22.17^\circ$ ,  $25.35^\circ$ ,  $29.94^\circ$ ,  $34.60^\circ$ ,  $37.57^\circ$ ,  $44.09^\circ$ ,  $47.08^\circ$ , and  $54.95^\circ$ , and the main peaks of the three groups of modified TPs modified with different concentrations of modifier were located at the same  $2\theta$  angles.  $\theta$  angle, and the intensity of the main peak did not change significantly, which indicates that the organic groups introduced by KH550 did not change the internal structure of TP, and only altered the surface properties of TP without affecting its own inherent physical properties.

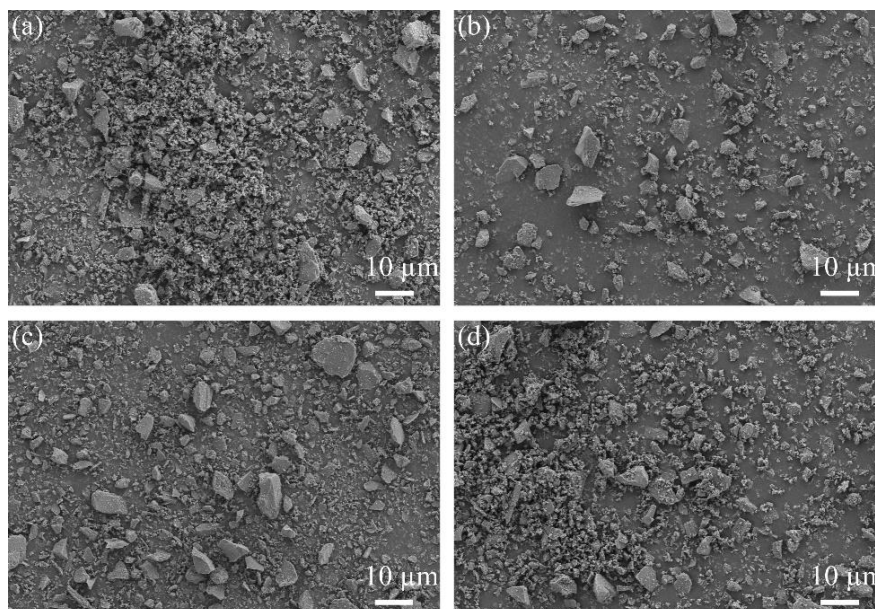


a-0% KH550-TP;b-1% KH550-TP;c-2% KH550-TP;d-3% KH550-TP

Figure 7: XRD patterns of TP modified with different concentrations of KH550 modifier

#### 4.1.4 SEM analysis

Figure 8 shows the SEM patterns of TP modified with different concentrations of KH550 modifier. Analyzing the SEM picture in Figure 8(a), there is obvious agglomeration phenomenon in the unmodified TP particles, and the powder particles are bonded with each other, the reason for this phenomenon is that TP is a material with large specific surface area and high specific surface energy, which is prone to agglomeration phenomenon due to its own polarization characteristics during the preparation and processing. In comparison with Fig. 8(b), it was found that the agglomeration phenomenon of TP powder modified by 1% concentration of KH550 was greatly reduced and the particles were uniformly dispersed, which indicated that the surface energy of TP particles was reduced and the dispersion of TP particles was effectively improved by the modification of organic modifiers. By comparing Fig. 8 (b) with Fig. 8 (c) and Fig. 8 (d), it was found that when the agglomeration phenomenon of TP particles was intensified with the increase of the concentration of the modifier, this was due to the fact that the excessive concentration of KH550 would lead to the formation of organosiloxane polymers on the surface of the TP particles by the unreacted hydrophilic groups, which would cause the TP particles to reaggregate<sup>[12]</sup>, which proved that 1% concentration of the KH550 modifier is the present experimental Optimal dosage.



a-0% KH550-TP; b-1% KH550-TP; c-2% KH550-TP; d-3% KH550-TP

Figure 8: Scanning Electron Microscope Images of Thermoplastic Modified with Different Concentrations of KH550 Modifier

## 4.2 Composite Material Analysis

### 4.2.1 Tensile test

Figure 9 shows the tensile strength of composites made with different KH550 modifier concentrations for different TP dosages. From Figure 9, it can be seen that when the TP doping is the same, the tensile strength of TP/PP composites after adding KH550 modifier is generally higher than that of the unmodified material, and the tensile strength decreases with the increase of modifier concentration; when the modifier concentration is the same, the tensile strength decreases with the increase of the TP doping; in which the composites made with 1% KH550-

TP at 10% (wt, mass fraction, the same hereinafter) have the optimum strength; the composites made under different KH550 modifier concentrations have the best tensile strength. The composites produced under the 10% (wt, mass fraction, the same below) dosage had an optimum tensile strength of 29.79 MPa, which was increased by 16.87% (31.23% compared with pure PP) compared with the unmodified control group with the same dosage.

The main reason for the improved tensile strength of the modified composites can be attributed to the fact that TP, as a material with a large specific surface area and high specific surface energy, is very prone to agglomeration during its preparation and processing, and the KH550 modifier improves the compatibility of the coated modified TP with PP materials, reduces the surface energy of tourmaline, improves its dispersion in PP, and forms a good bonding force with the matrix polymer at the interface; the KH550 modifier also improves the tensile strength of the coated TP. Good bonding; KH550 increases the interfacial bonding [13] and strength through the intertwining of its organophilic groups with PP molecular chains or the formation of weak hydrogen bonding, which enhances the tensile strength of the composite material. When the concentration of KH550 exceeds a certain amount, the tensile strength of the composites decreases. This is because the introduction of excess KH550 molecules leads to shorter molecular spacing and intermolecular hydrogen bonding between neighboring molecules, resulting in self-polymerization of KH550 molecules to form a chain or cluster structure and dehydration condensation between unreacted hydrophilic groups of reactive silanol groups (-Si-OH) to form a siloxane network, which results in the formation of micropores, interfacial phase separation, and areas of stress concentration inside the composites reducing the Tensile strength of the composites [14-16]. When the modified TP content exceeds a certain amount, the tensile strength of the composites also decreases. The reason for this phenomenon can be attributed to the incorporation of excessive modified TP, which is difficult to be dispersed by shear force during the extrusion process, resulting in uneven dispersion of modified TP in the PP matrix, discontinuity phenomenon at the interface, and an increase in the stress concentration point after the force is applied, so the addition of excessive modified TP leads to the decrease in strength [17].

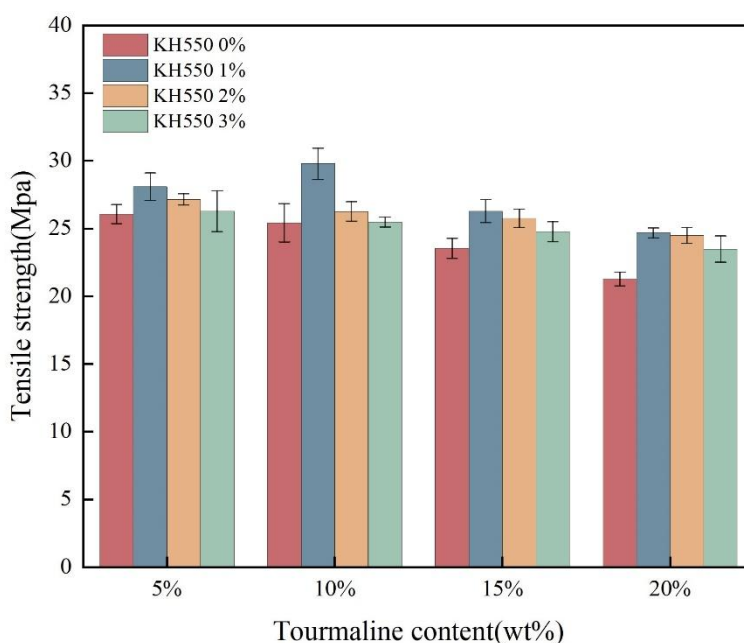


Figure 9: Tensile strength of TP/PP composites modified with KH550 at different modifier concentrations

#### 4.2.2 Bending test

Figure 10 shows the flexural strength of composites made with different KH550 modifier concentrations at different TP dosages. 1% concentration of KH550 modified TP at 5% dosage produced composite specimens with an optimal flexural strength of 44.22 MPa, compared to the unmodified 5% tourmaline powder dosage specimen flexural strength increased by 9.42% (compared to the pure PP improved by 15.2%), this group ratio is sufficient to improve the flexural strength of the modified TP/PP composites with different modifier concentrations. This ratio is enough to form a uniform, dense monomolecular chemisorption layer on the surface of tourmaline particles, and its amino end groups and alkyl long chains can physically entangle and interact with the PP matrix, thus constructing a strong interfacial phase between the inorganic filler and the organic polymer. This interface can effectively transfer the stress, so that the rigid filler bears the load, creating a transition layer capable of transferring and dispersing bending stresses (including tensile and compressive stresses), which effectively inhibits the generation of interface debonding and cracks on the tensile side, and improves the flexural strength of the composite.

As can be seen from Figure 10, when the TP doping is the same, the tensile strength of TP/PP composites after the addition of KH550 modifier is basically higher than that of the unmodified material, and the flexural strength decreases with the increase in the concentration of the modifier, the reason for the phenomenon is similar to the reason for the change in the tensile strength; when the flexural strength of 3% KH550-modified tourmaline with a doping of 5% is less than that of unmodified material, the reason for this is that the high concentration of modifier in the low doping of the composites, the flexural strength of the composites is lower than that of the unmodified material. The modifier in the low dosage of tourmaline powder surface formed more siloxane polymers, weakening the stress transfer efficiency, exacerbated the degree of TP agglomeration, so that the flexural strength is lower than the unmodified material, the same concentration of dosage increased to 10% after the phenomenon has been effectively mitigated, so with the increase in the dosage of modified TP in this concentration, the flexural strength will be improved.

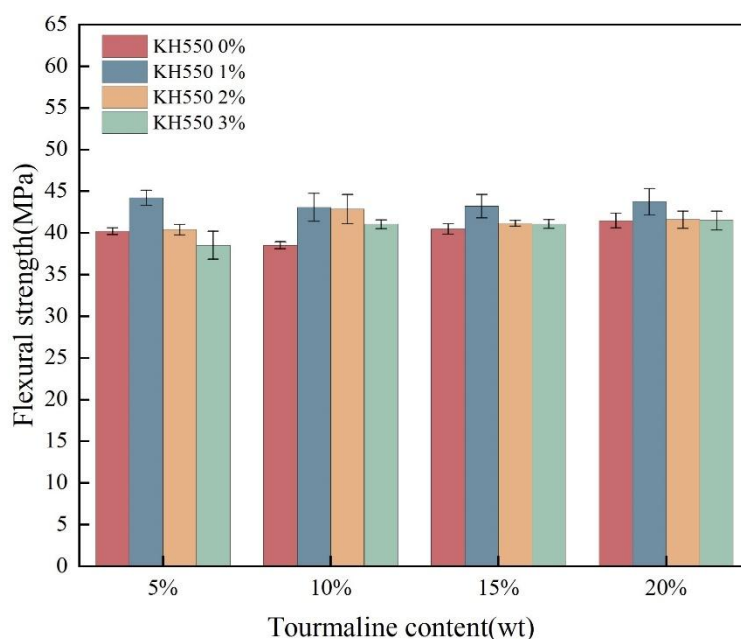
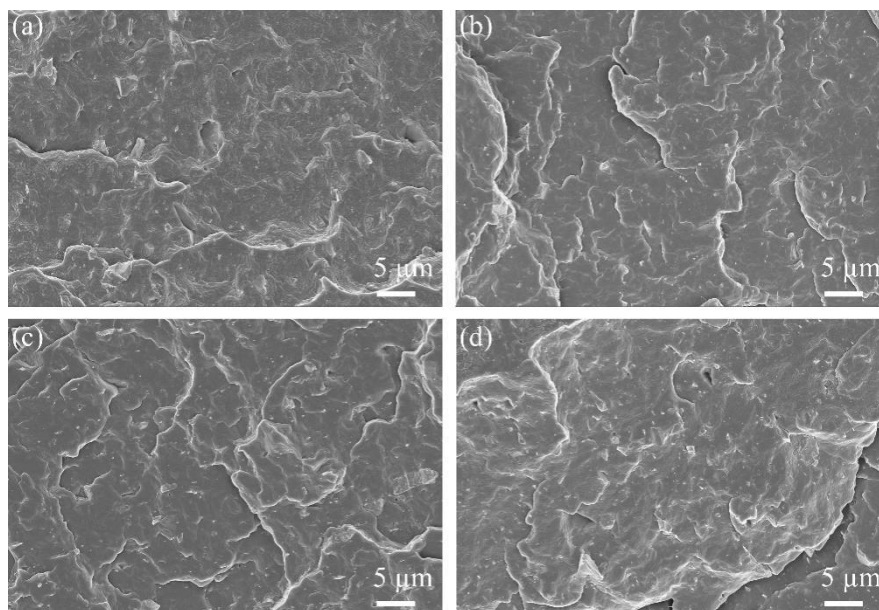


Figure 10: Flexural strength of TP/PP composites modified with KH550 at different modifier concentrations

### 4.2.3 SEM analysis

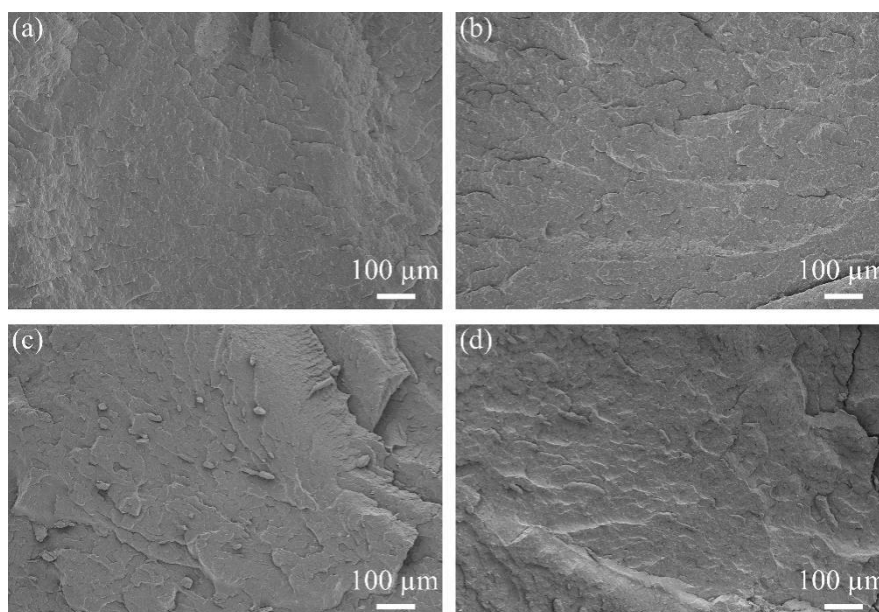
Figure 11 shows the SEM images of composites with different KH550 modifier concentrations and the same modified TP dosage (10 wt%). Due to the poor compatibility of the TP properties with the PP matrix, it can be seen in Figure 11(a) that there is an obvious demarcation line between the unmodified TP particles and PP matrix, which produces a concentration of stresses when the stress is applied, and TP particles are dislodged from the matrix to form an irregular cavity. In Fig. 11(b), it can be seen that after 1% concentration of KH550 treatment, the boundary between TP and PP matrix is blurred, the bonding is tight, and the number of irregular voids is reduced significantly, indicating that this concentration of KH550 improves the bonding strength between the two. KH550 treatment can form a bridge between TP and PP, and the hydrolysis of KH550 produces reactive silanol groups (-Si-OH), which can be combined with free hydroxyls of TP surface. The hydrolysis of KH550 produces reactive silanol groups (-Si-OH), which form (Si-O-Si)/(Si-O-M) covalent bonds with free hydroxyl groups (Si-OH)/(M-OH) on the surface of TP after the dehydration condensation, making the surface of TP wrapped by KH550, and the other end of the amino group (-NH<sub>2</sub>) and the alkyl group long-chain (-CH<sub>2</sub>-CH<sub>2</sub>-) can physically entangled and interacted with the PP substrate to improve the bonding strength between them. However, with the concentration of KH550, the bonding strength between the two can be improved. However, as the concentration of KH550 increases, the boundaries gradually clear and reappear irregular cavities, excess KH550 molecules make the intermolecular distance shorten, the neighboring active silanol groups (-Si-OH) dehydration condensation between the formation of siloxane network, this phenomenon will lead to KH550 molecules self-polymerization, the formation of a multilayer physically adsorbed interfacial weak layer on the surface of the TP, reducing the bonding strength of the TP and the PP matrix. bonding strength. This is one of the reasons why the mechanical strength of the composite material increases and then decreases with the concentration from 0% to 3%.

Figure 12 shows the SEM images of the composites with different modified TP doping at the same KH550 (1%) modifier concentration, in which a river-like pattern in the section can be observed, which is formed during brittle fracture as the crack meets the TP particles embedded in the PP matrix during the expansion process leading to the merging of bifurcations and steps, forming a pattern similar to the direction of the river [18]. With the increase of modified TP doping, the river-like pattern becomes more and more obvious, and obvious agglomerates can be observed in the cross-section pattern at 15 wt% doping [Fig. 12(c)] and 20 wt% doping [Fig. 12(d)], which is due to the fact that it is difficult to break up the excessive modified TP during extrusion, and modified TP is not dispersed homogeneously in the PP matrix, therefore, interfacial discontinuities and aggregation will occur. The phenomenon of discontinuity and agglomeration at the interface will occur, and the stress concentration point will be increased after the force is applied. On the macro level, the above reasons will lead to the decrease of mechanical properties when the doping of modified TP is increased by more than 15 wt%.



a-0% KH550-TP;b-1% KH550-TP;c-2% KH550-TP;d-3% KH550-TP

*Figure 11: Scanning electron micrographs of composite materials at different KH550 modifier concentrations and with the same modified TP content*



a-5wt% Modified-TP;b-10wt% Modified-TP;c-15wt% Modified-TP;d-20wt% Modified-TP

*Figure 12: Scanning electron microscope images of composite materials at different modified TP content levels with the same KH550 modifier concentration*

#### 4.2.4 TG analysis

Figure 13 shows the TG and DTG curves of the composites, where the inorganic fillers are all 10 wt% (KH550 concentration is 1%). From Fig. 13, it can be seen that the residual carbon rate of pure PP is 0.2% at 800°C, and the peak mass loss rate is reached at 448.3°C; the residual carbon rate of TP/PP composite is 8.7% at 800°C, and the peak mass loss rate is reached at 455.8°C; and the residual carbon rate of the KH550-TP/PP composite is 10% at time and the

peak mass loss rate is reached at 465.5°C. The TG and DTG curves of the composites are shown in Fig. 13, where the inorganic fillers are all 10 wt% (KH550 concentration is 1%). peak mass loss rate at 465.5°C. The above analysis shows that the addition of unmodified TP and modified TP improves the thermal stability of the composites, and the modified TP has the best effect.

The reasons for the incorporation of unmodified TP to improve the thermal stability are as follows, firstly, TP has its own polarization characteristics, when the ambient temperature rises, the molecular internal force will cause the strengthening of its own polarization effect, promoting the expansion and vibration of silicon-oxygen bond (Si-O-Si), boron-oxygen bond (B-O) and hydroxyl bond (-OH), and polar molecules are transformed from low-energy to high-energy, which will lead to the consumption of some of the energy, and the improvement of the thermal stability of the material[19, 20]. Secondly, because TP has thermoelectric properties, due to the anion in TP will generate electrostatic field when the temperature rises, the process of thermal energy will be converted into electrical energy to be consumed[21]. Thirdly, because of the negative ion release property of TP, the presence of anions in TP generates an electrostatic field on the surface not covered by PP, and when the DC electrostatic force comes into contact with water molecules, the water molecules are electrolyzed, and thus the heat will be further consumed[22]. Finally the presence of complex metal oxides in TP can catalyze the formation of a dense carbon layer, thus providing thermal and oxygen insulation[23]. Based on the above points, the incorporation of TP will improve the thermal stability of the composites.

KH550-TP is a surface modified TP made by grafting KH550 molecules on the surface of TP particles on the basis of unmodified TP, and the surface of TP will be wrapped by KH550. Since TP starts to decompose at 900-950°C, the decomposition temperature of KH550 is within 300-400°C. When the ambient temperature rises, the surface will be covered with KH550. When the ambient temperature rises, the KH550 molecules on the surface are the first to be decomposed, so its peak mass loss rate is greater than that of unmodified TP composites. When the KH550 molecules are decomposed, their internal chemical bonds are broken requiring the absorption of energy, and part of the heat is consumed. For the above reasons, the thermal stability of the composite is best after the addition of KH550-TP.

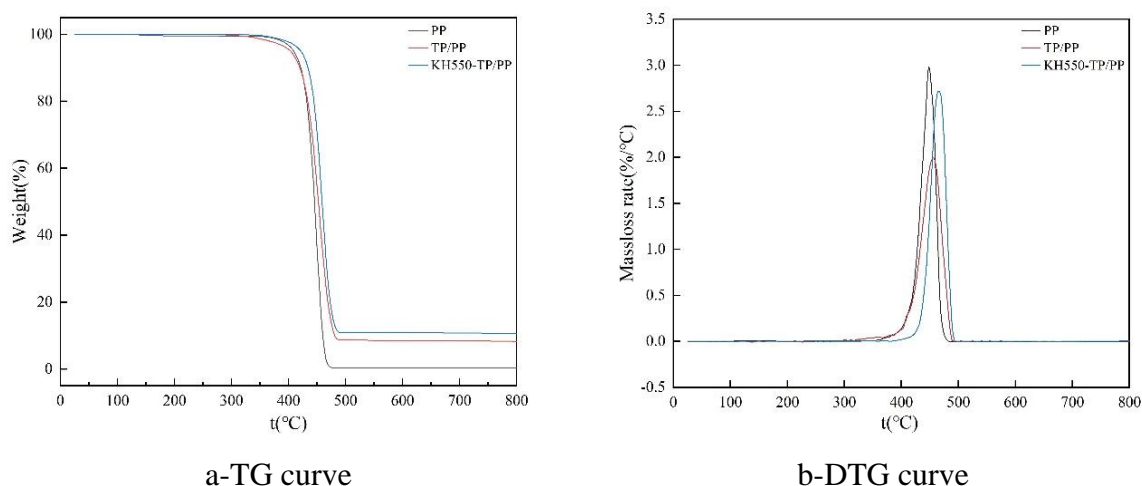


Figure 13: TG and DTG Curve Diagrams for Composite Materials

## 5 Conclusion

(1) KH550 can graft active groups on the surface of TP, which improved the agglomeration phenomenon of TP particles. 1% concentration of KH550 had the best modification effect, and

the contact angle of the modified TP increased from 10.86° to 41.78°, the hydrophobicity was significantly improved, and the dispersion of TP in the PP matrix and the degree of compatibility were improved.

(2) The optimum tensile and flexural strengths of modified TP/PP composites were obtained when the concentration of KH550 was 1%. The tensile strength of the composite was 29.79 MPa when the doping of modified TP was 10 wt%, which was 16.87% higher than that of the unmodified system; the flexural strength of the composite was 44.22 MPa when the doping of modified TP was 5 wt%, which was 9.42% higher than that of the unmodified system.

(3) Compared with the pure PP and TP/PP composite system, the KH550-TP/PP composite system has higher peak temperature of thermal decomposition and residual carbon rate, and shows good thermal stability.

## Funding

This work was supported by Department of Science and Technology of the Ningxia Hui Autonomous Region and the Research Fund of North Minzu University (2020KYQD40).

## References

- [1] da Silveira, P. H. P. M., Santos, M. C. C. d., Chaves, Y. S., Ribeiro, M. P., Marchi, B. Z., Monteiro, S. N., Gomes, A. V., Tapanes, N. d. L. C. O., Pereira, P. S. d. C., & Bastos, D. C. (2023). Characterization of thermo-mechanical and chemical properties of polypropylene/hemp fiber biocomposites: Impact of maleic anhydride compatibilizer and fiber content. *Polymers*, 15(15), 3271. <https://doi.org/10.3390/polym15153271>
- [2] Banu, R. D., Karunanithi, R., Sivasankaran, S., Subramanian, B., & Alhomidan, A. A. (2024). Synthesis, characterization, thermal and mechanical behavior of polypropylene hybrid composites embedded with CaCO<sub>3</sub> and graphene nano-platelets (GNPs) for structural applications. *AIMS Materials Science*, 11(3), 463-494. <https://doi.org/10.3934/matricsci.2024024>
- [3] Guo, M., Zhou, L., Dong, F., Zhang, W., Huo, T., Zhang, Y., Cao, Y., Xia, X., Manjoro, T. T., & Li, J. (2025). Gamma-ray irradiation engineering of tourmaline for medical-grade far-infrared mineral materials: Mechanistic insights and emissivity breakthrough. *Ceramics International*, 51(26), 50613-50620. <https://doi.org/10.1016/j.ceramint.2025.08.290>
- [4] Liu, Y., Rui, Y., Yu, B., Fu, L., Lu, G., & Liu, J. (2024). Study on the negative oxygen ion release behavior and mechanism of tourmaline composites. *Materials Chemistry and Physics*, 313, 128779. <https://doi.org/10.1016/j.matchemphys.2023.128779>
- [5] Zhao, Z., Wang, L., Lin, X., Xue, G., Hu, H., Ma, H., Wang, Z., Su, X., & Gao, Y. (2024). Effect of tourmaline addition on the anti-poisoning performance of MnCeO<sub>x</sub>@TiO<sub>2</sub> catalyst for low-temperature selective catalytic reduction of NO<sub>x</sub>. *Molecules*, 29(17), 4079. <https://doi.org/10.3390/molecules29174079>
- [6] He, J., Yu, X., Luan, X., Li, H., Shah, S. J., Su, W., Jia, Z., Chen, J., Zhou, L., Deng, J., Zhao, Z., Huang, Z., & Zhao, Z. (2024). Facile construction of tourmaline@MOFs

- composites via micron-scale electrical polarization to enhance photodegradation of gaseous formaldehyde. *Chemical Engineering Journal*, 479, 147828. <https://doi.org/10.1016/j.cej.2023.147828>
- [7] Wang, J., Wang, X., Zhou, P., Bian, L., & Wang, F. (2025). A simple fabrication of tourmaline-supported Ni-NiAl<sub>2</sub>O<sub>4</sub> nanocomposites for enhanced methane dry reforming activity. *Catalysts*, 15(7), 658. <https://doi.org/10.3390/catal15070658>
- [8] Zhang, Z., Sun, W., Huang, W., Zhu, Y., Li, J., Liang, C., & Gao, S. (2025). Interfacial and mechanical properties of silane coupling agent interface-modified basalt fiber reinforced thermoplastic polypropylene resin composites. *Polymer Composites*, 46(7), 6582-6593. <https://doi.org/10.1002/pc.29379>
- [9] Metanawin, S., Charoenchan, M., & Metanawin, T. (2024). The hemp-reinforced polypropylene composite: Effect of the alkaline and coupling agents treatment. *Journal of Elastomers & Plastics*, 56(5), 501-515. <https://doi.org/10.1177/00952443241252970>
- [10] Hu, Y., Liu, Y., Zheng, S., & Kang, W. (2024). Progress in application of silane coupling agent for clay modification to flame retardant polymer. *Molecules*, 29(17), 4143. <https://doi.org/10.3390/molecules29174143>
- [11] Wang, D., Liu, R., Wang, S., & Ma, X. (2024). Mechanical properties of ultra-high-performance concrete with amorphous alloy fiber: Surface modification by silane coupling agent KH-550. *Materials*, 17(16), 4037. <https://doi.org/10.3390/ma17164037>
- [12] Gao, J., Mei, J., Xiong, H., & Han, X. (2025). Effect of silane coupling agents on structure and properties of carbon fiber/silicon rubber composites investigated by positron annihilation spectroscopy. *Molecules*, 30(8), 1658. <https://doi.org/10.3390/molecules30081658>
- [13] Wu, Z., Li, C., Deng, Q., Liu, L., Teng, C., & Guo, P. (2025). Optimizing the compatibility of pyrolytic carbon black and asphalt interfaces using silane coupling agents: A cross-scale approach. *Case Studies in Construction Materials*, 23, e04996. <https://doi.org/10.1016/j.cscm.2025.e04996>
- [14] Ma, R., & Wang, S. (2025). Impact of APP modified with DOPO group-containing silane coupling agent on flame retardancy and mechanical properties of epoxy resin. *Journal of Applied Polymer Science*, 142, e57554. <https://doi.org/10.1002/app.57554>
- [15] Li, W., Du, W., Li, W., Chen, D., Liu, Y., & Ouyang, Y. (2023). Hygrothermal aging behavior and mechanical properties of modified ramie fiber reinforced polyethylene terephthalate glycol composites. *Cellulose*, 30(5), 3061-3072. <https://doi.org/10.1007/s10570-023-05064-4>
- [16] Reis, M. B., Carvalho, E. A. S., Delaqua, G. C. G., Azevedo, A. R. G., Monteiro, S. N., & Vieira, C. M. F. (2025). Analysis of the influence of coupling agents on the composition of artificial rocks with polymer matrix. *Scientific Reports*, 15, 32619. <https://doi.org/10.1038/s41598-025-18783-4>
- [17] Cavdar, A. D., Torun, S. B., Avci, B., & Mengeloglu, F. (2025). The engineering

- properties of polypropylene hybrid composites reinforced with lignin and zeolite. *Journal of Materials Research and Technology*. <https://doi.org/10.1016/j.jmrt.2025.08.100>
- [18] Haque, M. S., & Islam, M. A. (2024). Waste natural fibers for polymer toughening and biodegradability of epoxy-based polymer composite through toughness and thermal analysis. *Heliyon*, 10(6), e28110. <https://doi.org/10.1016/j.heliyon.2024.e28110>
- [19] Tang, X., Tang, R., Deng, Y., Li, X., Li, L., Zhou, Z., Li, W., Yuan, M., Xie, R., & Gong, D. (2024). Electric field driven tourmaline/hematite dual mineral photocatalysis for efficient antibiotic removal. *Environmental Pollution*, 352, 124135. <https://doi.org/10.1016/j.envpol.2024.124135>
- [20] Zhou, P., Han, X., Wu, L., Qi, M., Shen, Y., Nie, J., Liu, X., Wang, F., Bian, L., & Liang, J. (2025). Facile construction of novel BiOBr/black-TiO<sub>2</sub>/tourmaline composites for the synergistic degradation of tetracycline in aqueous solution. *Separation and Purification Technology*, 362, 131976. <https://doi.org/10.1016/j.seppur.2025.131976>
- [21] Qin, P., Zhang, Q., Xu, D., Sun, L., & Xie, X. (2024). Far-infrared radiation and therapeutic parameters: A superior alternative for future regenerative medicine? *Pharmacological Research*, 208, 107349. <https://doi.org/10.1016/j.phrs.2024.107349>
- [22] Wang, K., Wang, H., Zhang, S., Feng, X., & Zhao, Y. (2025). PES hemodialysis membrane possessing the function of releasing negative ions. *Journal of Materials Science*, 60, 9721-9742. <https://doi.org/10.1007/s10853-025-11016-z>
- [23] Cabello-Alvarado, C. J., Andrade-Guel, M., Perez-Alvarez, M., Cadenas-Pliego, G., Bartolo-Perez, P., Martinez-Carrillo, D., & Quinones-Jurado, Z. V. (2024). Green flame-retardant blend used to improve the ant flame properties of polypropylene. *Polymers*, 16(10), 1317. <https://doi.org/10.3390/polym16101317>